

Current-induced vortex unbinding in bolometer mixers

R. Barends^{a)}

Kavli Institute of NanoScience, Faculty of Applied Sciences, Delft University of Technology, Lorentzweg 1, 2628 CJ Delft, The Netherlands

M. Hajenius and J. R. Gao

Kavli Institute of NanoScience, Faculty of Applied Sciences, Delft University of Technology, Lorentzweg 1, 2628 CJ Delft, The Netherlands and SRON National Institute for Space Research, Sorbonnelaan 2, 3584 CA Utrecht, The Netherlands

T. M. Klapwijk

Kavli Institute of NanoScience, Faculty of Applied Sciences, Delft University of Technology, Lorentzweg 1, 2628 CJ Delft, The Netherlands

(Received 1 August 2005; accepted 3 November 2005; published online 27 December 2005)

We present a description of the current-voltage characteristics of hot electron bolometers in terms of the current-dependent intrinsic resistive transition of NbN films. We find that, by including this current dependence, we can correctly predict the complete current-voltage characteristics, showing excellent agreement with measurements for both low and high bias and for small as well as large devices. It is assumed that the current dependence is due to vortex-antivortex unbinding as described in the Berezinskii–Kosterlitz–Thouless theory. The presented approach will be useful in guiding device optimization for noise and bandwidth. © 2005 American Institute of Physics.

[DOI: 10.1063/1.2158510]

Phonon cooled hot electron bolometer (HEB) mixers have become the most suitable devices for low noise heterodyne detection above 1 THz. Using thin superconducting NbN films noise temperatures of 950 K at 2.5 THz and 1400 K at 2.8 THz have been obtained^{1,2} allowing actual use in astronomical instruments. Despite this recent technological progress an adequate understanding of the underlying physical mechanisms and a reasonable description of their current-voltage [$I(V)$] characteristics have not been reached yet. The standard picture of a HEB under operation is that due to radiation and bias the electrons in the NbN are heated and induce a local resistance, as follows from the temperature-dependent resistive transition of the superconducting material.^{3,4} The exact shape of temperature and resistivity profiles is ruled by a delicate interplay between thermal mechanisms, contact transmissivity, and the local resistivity.

Attempts to predict the current-voltage characteristics have been unsuccessful, leading to strong disagreement with the actual device response at the optimal operating point. This persistent discrepancy^{3,4} is indicative of a physical mechanism being absent in the current understanding of the HEB. In this letter we report the first model achieving full correspondence between predicted and measured current-voltage characteristics, using the measured current-dependent resistive transition of films used for lattice cooled HEBs. We will demonstrate that the $I(V)$ of the device can be understood as due to a local resistance generated by current-induced vortex unbinding, with the vortices acting as the source of resistance. An example of this approach is shown in Fig. 1, where the calculated $I(V)$ curves directly corre-

spond to the measured pumped curves of a small NbN HEB. For high bias as well as for low bias the predicted curves closely follow the measured ones. Typically the optimal operating point is around 0.5 mV. The method for calculating the $I(V)$ is presented below. We achieve similar results for larger devices.

Hot electron bolometers, consisting of a thin NbN film, can be as short as 150 nm and as narrow as 1 μm . They are coupled to Au antennas, with a NbTiN interfacial layer to maintain superconductivity of the contacts. The device is driven to its operating point by applying radiation from a local oscillator (LO) and by applying a dc voltage. It has

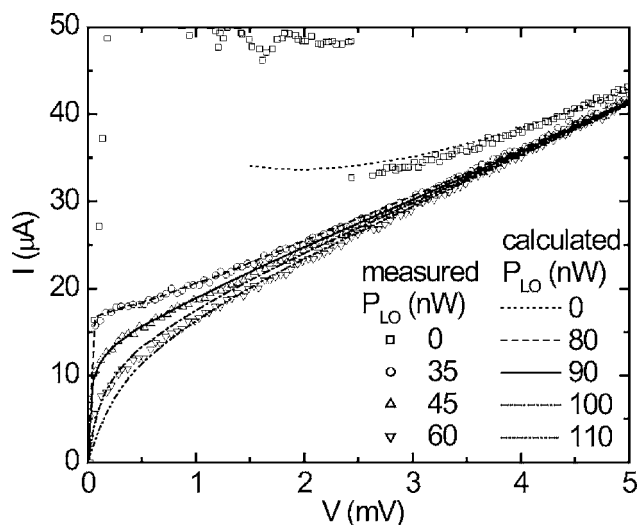


FIG. 1. Calculated current-voltage characteristics are compared to those of a small ($1 \times 0.15 \mu\text{m}$) device measured at 4.2 K with several local oscillator power (P_{LO}) levels at 1.6 THz. Using the current-dependent intrinsic resistive transition, the model correctly predicts $I(V)$, for high as well as low bias. Pumping power is determined using isothermal technique. The difference between pumping power needed for measurements and for calculations is attributed to uncertainties in the input parameters.

^{a)} Author to whom correspondence should be addressed; electronic mail: r.barends@tnw.tudelft.nl

been shown⁵ that under operating conditions the whole device, including the contacts, is in the superconducting state, except for the center of the NbN, where the resistance emerges due to the increase in the electron temperature. The Au antennas do not significantly contribute to the resistance and will be ignored. Hence, we will focus on the emergence of resistance in the NbN films used for the devices. It is known that flux flow and phase-slip events cause a voltage to appear in a superconductor at the onset of resistance.⁶ In thin superconducting films with a perpendicular penetration depth exceeding the coherence length this emergence can be understood in terms of vortex-antivortex unbinding according to the Berezinskii–Kosterlitz–Thouless theory.⁷ This theory has been appreciated in accounting for the excess noise accompanying the resistive transition⁸ and in transition edge sensor bolometers.⁹

The NbN films used are near the borderline of the superconductor-insulator transition due to their level of disorder and thickness as indicated by the sheet resistance.¹⁰ A full understanding of such a system has not been reached, although it is known to involve both quasiparticles (fermions) and vortices (bosons) in the presence of disorder.^{11,12} We assume that upon approaching the resistive state vortex-antivortex pairs exist below the Kosterlitz-Thouless temperature $T_{KT} < T_c$. Above this temperature free vortices emerge with a density N_F . The free vortices can move due to the Lorentz force, creating a time-dependent phase change, i.e., generating a voltage in the superconductor due to the Josephson relation. However, a current passing through the system contributes to the generation of free vortices by breaking the vortex-antivortex pairs.¹³ Hence, the resistance of the NbN film is in principle given by

$$R = R_N 2\pi\xi^2 N_F(J, T_e) \quad (1)$$

in which R_N is the normal state resistance, $2\pi\xi^2$ the area of a vortex core and $N_F(J, T_e)$ the density of free vortices, depending on the current density J and temperature T_e . Although the dissipation leads to a higher temperature of the electron and vortex system, denoted by T_e , the current breaks the vortex-antivortex pairs by the Lorentz force, even in the absence of a temperature rise. This is the *key assumption*, which we use to understand the current-voltage characteristics of the hot electron bolometer devices (their name being perhaps misleading).¹⁴

A full theoretical description is complicated by material properties, pinning sites, inhomogeneities, granularity, and finite-size effects. Instead we use an independently determined empirical relation for the resistive transition of the NbN film in the presence of a current. The intrinsic transition is measured for different dc current bias and shown in Fig. 2. The $R(T, I)$ curve shifts to lower temperatures for increasing current and the apparent downshift of the critical temperature T_c obeys the empirical relation

$$\frac{I}{I_c} = \left(1 - \frac{T_c(I)}{T_c(0)}\right)^\gamma \quad (2)$$

for $\gamma=0.54$, see the inset in Fig. 2. For different currents the $R(T)$ curve measured at small bias is taken with a shifted T_c . We ignore the small change in the steepness of the resistive transition for higher current bias.

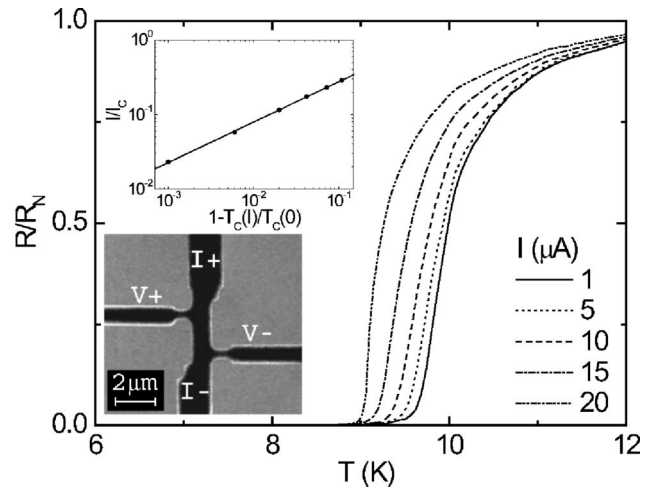


FIG. 2. The intrinsic resistive transition as a function of applied dc bias current of a 1- μm -wide processed NbN film. The film is dark in the scanning electron microscope image (lower inset) because it is covered by resist. The steepness changes little, while effectively the critical temperature, taken as the midpoint of the transition, shifts with increasing bias. This relation is depicted in the upper inset.

It is assumed that this empirical relation can be used as input to determine the current-voltage characteristics from the local resistivity ρ

$$V = J \int \rho(x, J, T_e(p_{LO}, p_{dc})) dx, \quad (3)$$

which depends on the current density and temperature. The temperature of the electron/vortex system is a result of the balance of local dissipation, heat transfer to the phonon bath and heat outflow into the equilibrium electrodes. So the *locality* of the resistance is due to the temperature profile, but the *value* of the local resistivity is set by both the temperature T_e and the current density J .

The specific shape of the temperature profile is determined from a one-dimensional distributed heat balance,^{3,4} which is formed by two coupled differential equations for the temperature T_e and the phonon temperature T_p

$$\begin{aligned} \frac{d}{dx} \left(\lambda_e \frac{d}{dx} T_e \right) + p_{dc} + p_{rf} - p_{ep} &= 0, \\ \frac{d}{dx} \left(\lambda_p \frac{d}{dx} T_p \right) + p_{ep} - p_{ps} &= 0, \end{aligned} \quad (4)$$

in which λ denotes a thermal conductivity, $p_{dc} = J^2 \rho$ is the locally generated dc power. The uniformly generated rf power is composed of the local oscillator and signal power, $p_{rf} = p_{LO} + p_s$. The power transfers between electron and phonon subsystems, and subsequently the substrate, are denoted by p_{ep} and p_{ps} . The temperature T_e dominates the device response over the phonon temperature.

The one-dimensional approach is motivated by the skin depth and the magnetic penetration depth being larger than or of the same magnitude as the device width. Since $hf \gg 2\Delta$ the rf power absorption is assumed to be uniform, following Ref. 15. We assume full thermalization because the inelastic electron-electron interaction length, typically around 10 nm, is smaller than the device length. The electron-phonon interaction time being smaller than the phonon escape time, $\tau_{ep} < \tau_{esc}$, and the wavelength of a thermal

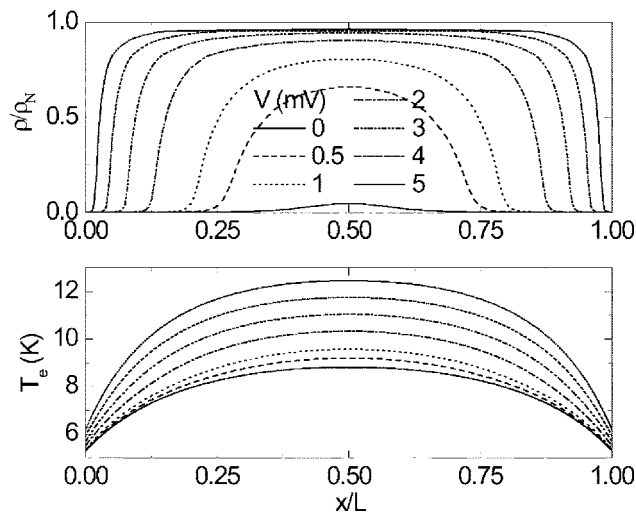


FIG. 3. Local resistivity and temperature profiles for the same device as in Fig. 1 at $P_{LO}=90$ nW (optimal power) for different dc bias voltages, calculated using the current-dependent intrinsic resistive transition and Eq. (4). The voltage bias for the optimal operating point is typically 0.5 mV. The currents associated with the bias voltages can be inferred from Fig. 1.

phonon, typically around 20 nm, being smaller than the device length, motivates the use of the phonon temperature. See Ref. 16 for further details.

The temperature and local resistivity profiles are shown in Fig. 3. The bias current and the LO power induce temperature profiles which translate into bell-shaped resistivity profiles. Clearly the device response in the optimal operating point is dominated by the center of the bolometer, indicated by the strong rise for increasing bias. Mixing occurs therefore in this region. Using the local resistivity as shown in Fig. 3, we are able to fully describe the measured current-voltage characteristics in Fig. 1.

To conclude, we have identified current as a dominant player in the intrinsic resistive transition. Using this current-dependent resistivity criterion we achieve full correspondence between predictions and measurements. A systematic study of the current dependence within the context of the Berezinskii–Kosterlitz–Thouless transition is needed. This

sheds a new light on the notion of mixing mechanisms and time-dependent processes related to the thermal time constants. It will also influence the noise properties,⁸ which might hint at the possibility of excess noise in HEB mixers, analogous to the excess noise in transition edge sensors.⁹

We thank A. Baryshev for stimulating discussions and J.J.A. Baselmans for also making available the measured $I(V)$ data. The work is supported partly by RadioNet and partly by INTAS.

¹J. R. Gao, J. N. Hovenier, Z. Q. Yang, J. J. A. Baselmans, A. Baryshev, M. Hajenius, T. M. Klapwijk, A. J. L. Adam, T. O. Klaassen, B. S. Williams, S. Kumar, Q. Hu, and J. L. Reno, *Appl. Phys. Lett.* **86**, 244104 (2005).

²J. J. A. Baselmans, M. Hajenius, J. R. Gao, T. M. Klapwijk, P. A. J. de Korte, B. Voronov, and G. Gol'tsman, *Appl. Phys. Lett.* **84**, 1958 (2004).

³P. Khosropanah, Ph.D. thesis, Chalmers University of Technology, 2003.

⁴T. M. Klapwijk, R. Barends, J. R. Gao, M. Hajenius, and J. J. A. Baselmans, *Proc. SPIE* **5498**, 129 (2004).

⁵M. Hajenius, R. Barends, J. R. Gao, T. M. Klapwijk, J. J. A. Baselmans, A. Baryshev, B. Voronov and G. Gol'tsman, *IEEE Trans. Appl. Supercond.* **15**, 495 (2005).

⁶M. Tinkham, *Introduction to Superconductivity* (McGraw-Hill, New York, 1996).

⁷M. R. Beasley, J. E. Mooij, and T. P. Orlando, *Phys. Rev. Lett.* **42**, 1165 (1979).

⁸R. F. Voss, C. M. Knoedler, and P. M. Horn, *Phys. Rev. Lett.* **45**, 1523 (1980).

⁹G. W. Fraser, *Nucl. Instrum. Methods Phys. Res. A* **523**, 234 (2004).

¹⁰H. Su, N. Yoshikawa, and M. Sugahara, *Supercond. Sci. Technol.* **9**, A152 (1996).

¹¹V. M. Galitski, G. Refael, M. P. A. Fisher, and T. Senthil, *cond-mat/0504745*.

¹²A. M. Goldman and N. Markovic, *Phys. Today*, **51**, 39 (1998).

¹³A. M. Kadin, K. Epstein, and A. M. Goldman, *Phys. Rev. B* **27**, 6691 (1983).

¹⁴In earlier work the current dependence has been considered but in a different way than applied here. See A. I. Elantiev and B. S. Karasik, *Sov. J. Low Temp. Phys.* **15**, 379 (1989); R. S. Nebosis, A. D. Semenov, Yu. P. Gousev, and K. F. Renk, *Proceedings of the Seventh International Symposium on Space THz Technology, 1996*, p. 601, and Ref. 3.

¹⁵B. S. Karasik and A. I. Elantiev, *Appl. Phys. Lett.* **68**, 853 (1996).

¹⁶R. Barends, M. Hajenius, J. R. Gao, and T. M. Klapwijk, *Proceedings of the 16th International Symposium on Space THz Technology, 2005*.